

Anatomy of skin modes and topology in non-Hermitian systems

Ching Hua Lee^{1,2,*} and Ronny Thomale³

¹*Institute of High Performance Computing, A*STAR, Singapore, 138632.*

²*Department of Physics, National University of Singapore, Singapore, 117542.*

³*Institute for Theoretical Physics and Astrophysics,
University of Würzburg, Am Hubland, D-97074 Würzburg, Germany*

(Dated: June 22, 2022)

A non-Hermitian system can exhibit *extensive* sensitivity of its complex energy spectrum to the imposed boundary conditions, which is beyond any known phenomenon from Hermitian systems. In addition to topologically protected boundary modes, macroscopically many “skin” boundary modes may appear under open boundary conditions. We rigorously derive universal results for characterizing all avenues of boundary modes in non-Hermitian systems. We show, for the first time, how the exact energies and decay lengths of skin modes can be obtained by threading an imaginary flux. Secondly, we also derive a novel and very straightforward criterion for the existence of generic 1D topological boundary modes which does not require a contour specifically tailored to the system at hand. It also reveals that the topologically nontrivial phase is partitioned into regions where the boundary mode decay length depend differently on complex momenta roots. These results generalize known winding number approaches that are not necessarily valid beyond the simplest models, and are intimately based on the complex analytical properties of in-gap exceptional points.

The avenue of topological phases has reshaped our perspective on single-particle problems in condensed matter physics [1–3]. Unlike interacting many-body problems which are seldom exactly solvable, single-particle problems are often naively conceived as conveniently tractable on mostly analytic grounds, with its quantum and classical realizations treatable on equal formal footing. This view, however, underestimates the richness and intricacies from the structure of phase and parameter space of the given physical system [4], as well as the added complexity implied by the investigation of boundary terminations [5], external driving [6], and open systems beyond the realm of Hermiticity [7].

Non-Hermiticity can arise not just from the inherent gain or loss in a system, but also from non-reciprocity. Such non-Hermitian influences are particularly interesting, exhibiting as many exciting new phenomena as the fundamental challenges they pose in their characterization. For instance, complex energy bands can develop branch cuts terminating at so-called exceptional points [8–15] that can extend along loops [16–18], and bulk modes can morph into boundary “skin” modes with large densities of states [10, 19]. It is a fascinating, yet poorly understood, task to understand how non-Hermiticity conspires with topology. In a topologically non-trivial Hermitian lattice system, a boundary termination only introduces a sub-extensive number of in-gap modes protected by eigenmode topology. The bulk states, being delocalized, remain largely undisturbed. By contrast, in a non-Hermitian system, the *entire* spectrum of an arbitrary large system can be modified by introducing a boundary, ostensibly violating the usual bulk boundary correspondence [10, 19–23].

As we shall analytically elucidate, this seemingly counterintuitive sensitivity to boundary conditions is but one

consequence of the fundamental observation that local perturbations of a non-reciprocity system can drive it into essentially *different* phases, each with its distinct exceptional points and winding numbers. This is because non-Hermitian eigenmodes generically become spatially (exponentially) localized whenever there is non-reciprocity. Indeed, there are two types of non-Hermitian boundary eigenmodes: Extensive skin modes, which, as we show, can be continuously interpolated from Hermitian bulk modes through analytic continuation and, subextensive topological boundary modes, which are protected by a new non-Hermitian topological winding number criterion that does not require a contour specifically tailored to the particular system.

Recent attempts at characterizing these enigmatic boundary modes have not always been conclusive. Even after generalizing topological quantities such as the Berry curvature and the Chern number to their biorthogonal non-Hermitian analogs [13, 23–25], there remain difficulties in choosing the most appropriate and efficient quantities for capturing phase transition jumps [25]. While Refs. [21] and [22] have identified jumps in the biorthogonal polarization as necessary conditions for topological phase transitions, it remains unclear when they are also sufficient, an observation which only reveals itself as one investigates more general non-Hermitian models beyond the simplest examples. Quantitative predictions of the localization lengths and dispersions of skin modes are even more elusive, with existing results being mostly restricted to numerical studies or fine-tuned models where boundary modes can be calculated exactly [10, 19, 22, 23]. A few key outstanding questions thus are: (i) Some non-Hermitian systems are extremely sensitive to boundary conditions (skin effect), while others are not. What conditions are not just necessary but also *sufficient* for the

non-Hermitian skin effect? (ii) When skin modes appear, how can one compute their energy dispersions, densities of states, and localization lengths? (iii) Can we formulate a topological criterion that determines, without prior knowledge of complex band touching locations, the existence of topological boundary zero modes? In this work, we settle these questions through a universal treatment of boundary modes in non-Hermitian systems.

Complex flux for characterizing skin modes – Usually, open boundaries break translational invariance and preclude exact analytic characterization of the consequent eigenmodes. In the special case of skin modes, however, it turns out that we can obtain analytical results via a mode pumping argument [26–31] with *complex* fluxes. We treat a generic lattice system as a collection of 1D

chains perpendicular to the open boundary, with coordinates of other dimensions taken as external parameters. Consider a 1D chain described by a Hamiltonian $H = \sum_{n=-N_L}^{N_R} \sum_x T_n c_x^\dagger c_{x+n} = \sum_{n=-N_L}^{N_R} \sum_k e^{ikn} T_n$, such that a hopping across a displacement of n unit cells (i.e. sites) is given by the matrix T_n . We assume reasonably local hoppings, so $N_L, N_R \sim O(1)$. Under periodic/open boundary conditions (PBCs/OBCs), the chain can be visualized as a ring with hoppings present/absent across its endpoints. Via Faraday’s law, flux can threaded through this ring by shifting the momentum k via minimal coupling $k \rightarrow k + \phi$, where $\dot{\phi}$ is the rate of change of flux which equals the induced (fictitious) electromagnetic field. Equivalently, this flux multiplies each hopping with a phase factor viz. $T_n \rightarrow T_n e^{in\phi}$.

To relate this flux pumping with the boundary conditions (BCs), one performs a gauge transformation $H \rightarrow V^{-1} H V$ with $V = \text{diag}(e^{-i\phi}, e^{-2i\phi}, \dots, e^{-il\phi})$, l being the system length. This removes the phase from all the hoppings except for those across the endpoints, which acquire a phase of $e^{\mp il\phi}$. Through this, we have managed to re-express BCs on the boundary hoppings in terms of *translationally-invariant* fluxes.

We next construct an interpolation between PBCs and OBCs for studying how non-Hermitian skin modes arise. For that, we have to first introduce the *semi-open* boundary condition (semi-OBC), which has the boundary hoppings vanish in one direction but not the other. This is necessary because an imaginary flux component will always produce a rescaling factor $O(e^{l\text{Im}\phi})$ that diverges with l at one of the boundaries. For definiteness, we set hoppings $T_{n<0}|_R$ from the right to the left boundary to zero, but preserve their reciprocal hoppings $T_{n>0}|_L$. As ϕ becomes complex, $T_{n>0}|_L$ will be rescaled by a factor of $e^{-l\text{Im}\phi}$. When $\text{Im}\phi = 0$, we have perfect PBC in one direction; as $\text{Im}\phi \rightarrow \infty$, we approach the OBC limit. Hence, to find the spectrum of $H(k)$ under the semi-OBC of $T_{n>0}|_R = 0$ and $T_{n>0}|_L$ rescaled by a factor $e^{-\kappa l}$, which tends to the exact OBC when $\kappa l \rightarrow \infty$, we can simply diagonalize the *translationally invariant* analytic continuation of the original Hamiltonian:

$$H_\kappa(k) = H(k + i\kappa), \quad (1)$$

which possesses an identical spectrum as the semi-OBC system. To anticipate upcoming notation, we define $z = e^{ik}$, $k \in \mathbb{C}$. Physically, (1) implies that all the original PBC bulk states *must* morph into left boundary modes with localization lengths κ^{-1} under this semi-OBC. Furthermore, $H_\kappa(k) \forall \kappa$ forms an equivalence class of Hamiltonians with identical OBC spectra. Such macroscopic condensation of modes onto one edge does not happen in Hermitian systems because semi-OBCs, being non-

reciprocal, destroy hermiticity, and as such is a physically unrealistic proxy for OBC. But for the skin modes, OBCs and (correctly chosen) semi-OBCs are essentially equivalent, since the BCs are only consequential at the boundary where the skin mode is localized. Henceforth, we shall no longer distinguish OBCs from semi-OBCs in this work.

The above developments allow us to understand why superficially similar systems may manifest markedly different non-Hermitian effects. We illustrate this insight using the example of the generalized non-Hermitian Su-Schrieffer-Heeger (SSH) model [10, 21, 22, 32, 33]:

$$H_{\text{SSH}}^{\gamma_x, \gamma_y}(k) = \left(\frac{1}{2} + \cos k\right) \sigma_x + \sin k \sigma_y + i\gamma_x \sigma_x + i\gamma_y \sigma_y, \quad (2)$$

where σ_x, σ_y denote the Pauli matrices. As shown in Fig. 1, $H_{\text{SSH}}^{\gamma, 0}$ and $H_{\text{SSH}}^{0, \gamma}$ possess qualitatively different behavior as PBCs are morphed into OBCs via imaginary flux ($\text{Im}\phi$) pumping. $H_{\text{SSH}}^{\gamma, 0}$ (Fig. 1a-c) respects the usual BB-correspondence, with its OBC and PBC spectra coinciding except for isolated topological boundary modes, while for $H_{\text{SSH}}^{0, \gamma}$ (Fig. 1d-f) almost *all* the bulk modes collapse into boundary skin modes in the imaginary flux evolution towards the OBC limit. Empirically, it appears that PBC bulk modes (red in Fig. 1b,c,e,f) tend to evolve into the interior of their PBC loci, and will not move (and hence obey the BB correspondence) only if they already lie along an open arc, which is the case only for $\gamma_y = 0$. Below, we shall uncover exactly how we can explain the trajectories of PBC-OBC spectral flows, and how the energies and dispersions of their endpoints (OBC skin modes) can be analytically determined.

OBC constraints and skin mode solutions – Naively, one may be tempted to find the skin modes by simply taking the $\kappa \rightarrow \infty$ exact OBC limit. This, however, would yield undetectable modes with vanishing decay lengths. To correctly find the skin modes of a Hamilto-

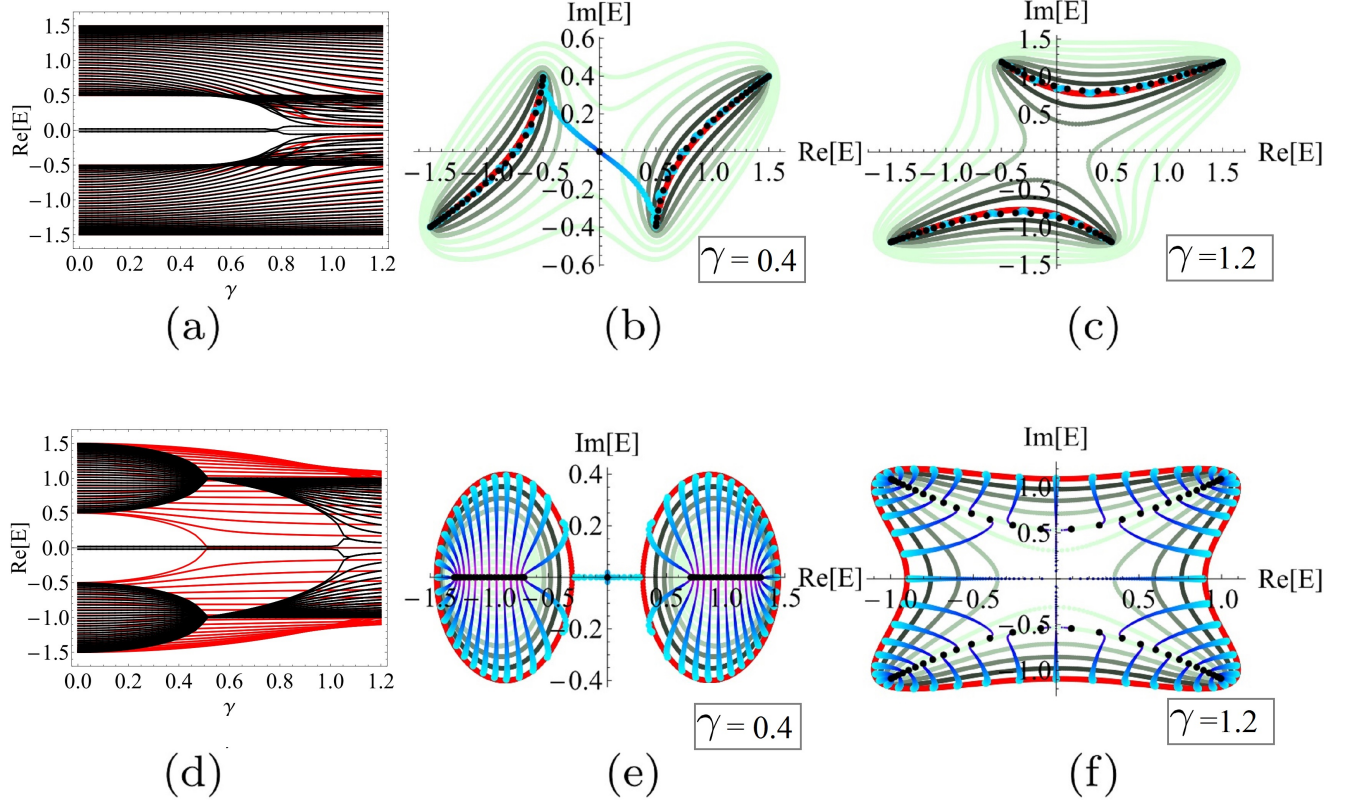


FIG. 1: Qualitatively distinct spectra for $H_{\text{SSH}}^{\gamma,0}$ (a-c) and $H_{\text{SSH}}^{0,\gamma}$ (d-f) from Eq. 2. (a,d): Both systems exhibit topological zero modes (black lines at $\text{Re}[E] = 0$) for sufficiently small non-Hermiticity γ , but only $H_{\text{SSH}}^{\gamma,0}$ exhibits the usual bulk boundary correspondence. For $H_{\text{SSH}}^{0,\gamma}$, all the OBC (black) modes differ from the PBC (red) modes, not just for the topological boundary modes. (b,c,e,f): Anatomy of PBC and OBC spectra in the complex energy plane for both models, for both topologically nontrivial ($\gamma = 0.4$) and trivial ($\gamma = 1.2$) cases. The light blue/magenta tapering curves illustrate the evolution trajectories of the PBC modes into OBC modes as $\text{Im} \phi$ increases from 0 to ∞ . For $H_{\text{SSH}}^{\gamma,0}$ (b,c), the PBC and OBC spectra both lie along the same open arcs and no imaginary flux evolution is visible, except for an isolated zero mode in b). For $H_{\text{SSH}}^{0,\gamma}$ (e,f), however, the OBC creates skin modes (black) which morphed en-masse from the PBC modes (red), retaining no resemblance of their original loci. The background light blue closed curves are contours of constant $\kappa = \text{Im} k$ with intervals of 0.1; bulk modes become localized skin modes as soon as they lie along $\kappa \neq 0$ contours. Note that from Eq. 7, one can show that the skin modes (black) of (f) occur along points of $\text{Re}[z^2] = \frac{5}{4} - \gamma_y^2$ satisfying $4\gamma_y^2 > 1 + (\text{Im}[E^2])^2$.

nian $H(z) = H(e^{ik})$, we construct the ansatz mode $\psi(x)$ from the subset of its Hilbert space with eigenenergy E :

$$\psi(x) = \sum_{\mu} c_{\mu} \beta_{\mu}^x \varphi_{\mu}, \quad (3)$$

$$E \varphi_{\mu} = H(\beta_{\mu}) \varphi_{\mu}, \quad (4)$$

where the set of β_{μ} 's consist of all the roots of the characteristic polynomial $\text{Det}[H(z) - E \mathbb{I}] = 0$, where E is considered a fixed parameter. Note that the index μ , as defined, repeatedly runs over the same eigenvectors because the number of roots β generically exceeds $\dim H$. The bulk Hamiltonian specifies that

$$H\psi(x) = \sum_{-N_L < n < N_R; \mu} c_{\mu} \beta_{\mu}^{x+n} T_n \varphi_{\mu} = E\psi(x), \quad (5)$$

which is satisfied for any set of c_{μ} 's. Beyond that, the OBC places additional constraints stipulating that the mode $\psi(x)$ must vanish outside $x \in [0, l]$. Specifically, at every site $x_L(x_R)$ within $N_L(N_R)$ sites from the left(right) edge, hoppings beyond the edge should be truncated from the Hamiltonian. Subtracting these boundary truncations for $0 < x_L \leq N_L$ and $0 < x_R \leq N_R$ from Eq. 5, we obtain the following $N_L + N_R$ constraints for the left and right boundaries, respectively:

$$\begin{aligned}
\sum_{x_L \leq n \leq N_L} z^{-n} T_{-n} \psi(x_L)|_{z=\beta} &= \sum_{x_L \leq n \leq N_L; \mu} c_\mu \beta_\mu^{x_L-n} T_{-n} \varphi_\mu = 0, \\
\sum_{x_R \leq n \leq N_R} z^n T_n \psi(l-x_R)|_{z=\beta} &= \sum_{x_R \leq n \leq N_R; \mu} c_\mu \beta_\mu^{l-x_R+n} T_n \varphi_\mu = 0,
\end{aligned} \tag{6}$$

which collectively determine the coefficients c_μ . Notably, in the thermodynamic limit of large l , only the term/s with the largest $|\beta_\mu|$ survive in Eq. 6. Yet, generically there cannot be a unique largest $|\beta_{\mu_{max}}|$ if $\varphi_{\mu_{max}}$ were to survive, since none of the other terms would be large enough to cancel off the $c_{\max} \beta_\mu^l$ term as $l \rightarrow \infty$. Exceptions occur when Eqs. 6 is not full rank due to some fortuitous redundancies in the $T_{\pm n} \varphi_\mu$'s; such isolated cases will be revealed as “topological” modes later. Hence we conclude that for any non-topological bulk or skin boundary mode to exist, a *necessary* condition is that:

$$\exists \mu \neq \nu \text{ such that } |\beta_\mu| = |\beta_\nu|. \tag{7}$$

Eq. 7 has previously appeared in Refs. [21] and [22] as the condition for an extended bulk state, where a topological phase transition leads to a biorthogonal polarization jump[22]. Through our derivations, however, Eq. 7 has far broader, hitherto unappreciated consequences: It is the condition for *any* non-topological mode to exist under OBCs, be they bulk or skin modes. It holds even for usual Hermitian systems, where all bulk eigenmodes trivially fulfill $|\beta_\mu| = 1$.

As such, necessary *and* sufficient conditions for boundary skin modes can be obtained by letting the imaginary flux κ in Eq. 1 evolve from 0 to $\pm\infty$, stopping when Eq. 7 is satisfied for the first time. In order to appreciate the depth of this finding, we need to investigate slightly generalized models as compared to (2). Specifically, we analyze a class of minimal Hamiltonians $H_{\min}(z)$ in which the full complexity of non-Hermitian spectral flow unfolds:

$$H_{\min}(z) = \frac{9}{4} \sigma_x - 3z \sigma_- + 3 \left(1 - \frac{1}{z} - \frac{1}{z^2} \right) \sigma_+, \tag{8}$$

where $\sigma_\pm = (\sigma_x \pm i\sigma_y)/2$. The spectrum, and its evolution in the complex plane, is depicted in Fig. 2a-c. Generically, the eigenenergies, i.e., eigenmodes flow towards the interior of the PBC energy contour (red), stopping only if they collide with other modes (black). Since these collisions occur for eigenenergies with the same κ , they must be solutions where the β s with $e^{-\kappa} = |\beta|$ coincide (Eq. 7). Saliiently, not all solutions of equal $|\beta|$ correspond to skin modes - only those with largest $|\beta|$ i.e. smallest $|\kappa|$ will be visited by the spectral evolution, and hence exist as OBC eigenmodes. All these findings, are not specific to this particular model, and hold for arbitrarily complicated Hamiltonians, as illustrated for another model in Fig. 2d.

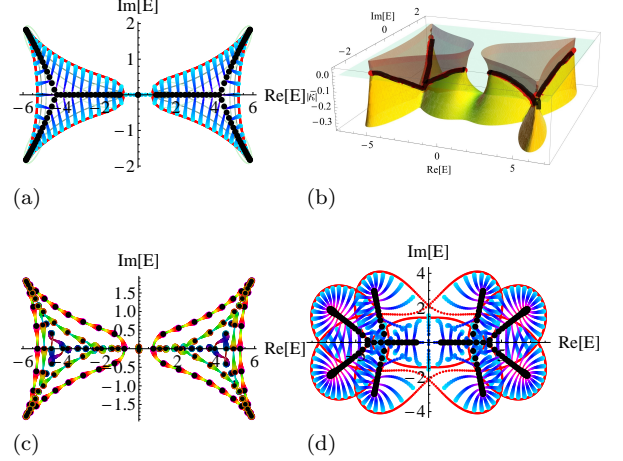


FIG. 2: (a-c) PBC-OBC spectral flow of model (8). In a), PBC bulk eigenvalues (red) flow along the blue-purple curves, accumulating along the Y-shaped black lines as OBC skin modes. These black lines are the largest magnitude solutions to $|\beta_\mu| = |\beta_\nu|$ (Eq. 7), as evident from the light blue background contours of spacings $|\Delta\kappa| = \Delta \log |\beta| = 0.07$. This flow can be more concretely visualized in the complex energy vs. κ plot of b), where the Y shape (black) emerges at the intersection of the two solutions (brown and yellow) of $|\beta| = e^{-\kappa}$ closest to the real plane $|\beta| = 1$ (blue). The eigenmodes “slide down” the brown surface upon imaginary flux threading, till they stop along the black valley. c) illustrates eigenmodes flowing into each other under the threading of a real flux $\text{Re } \phi \rightarrow \text{Re } \phi + 2\pi/l$, tracing successively smaller loops as the boundary hopping $e^{-l\kappa}$ diminishes with increasing κ (Shown are $\kappa = 0, 0.16, 0.25$). d) Demonstration of the imaginary flux argument for an extended minimal model $H_{\min}(k) + 4z^{-3}\sigma_-$ with more convoluted arcs.

To understand why the eigenmodes should converge along (exceptional) points or arcs in the OBC limit, we consider their spectral flow upon threading of the *real* part of a flux: $\phi = \text{Re } \phi + i\text{Im } \phi \rightarrow (\text{Re } \phi + 2\pi/l) + i\text{Im } \phi$. This corresponds to multiplying the boundary hopping by a suppression factor with rotating phase: $e^{-l\text{Im } \phi} \rightarrow e^{-l\text{Im } \phi} e^{2\pi i}$. This evolution corresponds to a permutation of the eigenmodes, since $e^{2\pi i} = 1$. But evidently, its physical significance should vanish in the OBC limit of large $\text{Im } \phi$, since there will be no more boundary hopping to be rotated! As such, we intuitively expect the spectrum to contract into smaller and smaller loops when approach-

ing the OBC limit, halting when the loops degenerate into arcs or isolated exceptional points that exist only under OBCs and not PBCs. Hamiltonians which do not host skin modes are precisely those whose PBC spectra already are located along an arc. This includes all Hermitian systems, with spectra confined to the real line, as well as *reciprocal* non-Hermitian systems, whose symmetric hoppings ($T_n = T_{-n}^T$) force the PBC spectrum to retrace itself. (Note that up to now, those are the models that have predominantly been realized in experimental setups.)

Criterion for non-Hermitian topological phases – Besides the continuum of skin boundary modes that connect analytically to Hermitian bulk modes, there can also exist isolated “topologically protected” boundary zero modes.

Below, we shall derive a novel criterion for the existence of such zero modes protected by particle-hole (PH) symmetry (Eq. 15) that generalizes previous invariants for non-Hermitian systems from Refs. [21, 22, 25, 33], and is straightforward to apply even for arbitrarily complicated models. In the context of OBC constraints (Eqs. 6), “topological” modes occur at special points where the system formed by Eqs. 6 is not of full rank, such that the eigenmode weights c_μ have nonzero solutions *despite* $|\beta_\mu| \neq |\beta_\nu|$ for any pair μ, ν . Rewriting Eqs. 6 as a matrix equation $M\mathbf{c} = \mathbf{0}$, this condition for a topological mode translates to $\text{Det } M = 0$. Noting that rescaling the square root denominators does not change the topology, we consider the most generic PH symmetric 2-component Hamiltonian given by

$$H^{\text{PH}}[\{r_{a/b}\}; \{p_{a/b}\}](z) = \begin{pmatrix} 0 & a(z) \\ b(z) & 0 \end{pmatrix} = \begin{pmatrix} 0 & z^{r_a} \prod_i^{p_a} \frac{(z-a_i)}{z\sqrt{a_i}} \\ z^{r_b} \prod_i^{p_b} \frac{(z-b_i)}{z\sqrt{b_i}} & 0 \end{pmatrix}, \quad (9)$$

where a_i, b_i are the complex roots of $a(z), b(z)$. The exceptional nature of the $E = 0$ in-gap point turns out to be key in expressing $\text{Det } M = 0$ as a constraint on winding numbers. Exactly at $E = 0$, either $a(z)$ or $b(z)$ vanishes and the $p_a + p_b$ roots β_μ correspond to the a_i ’s or b_i ’s, with corresponding eigenmodes $(1, 0)^T$ or $(0, 1)^T$. For any finite system size l , however, the topological mode is displaced from zero by $E \sim e^{-l}$, and the φ_μ will acquire $O(E)$ corrections. To be explicit, let us specialize to the simple, but still sufficiently rich case of $p_a = p_b = 2$ and $r_a = r_b = 1$, such that there are $p_a + p_b = 4$ eigenmodes. The Hamiltonian is a generalized SSH model with complex coefficients and phases:

$$H_{\min}^{\text{PH}}(z) = [\alpha_+ \cos k + i\alpha_- \sin k - \alpha_0] \sigma_+ + [a_i \leftrightarrow b_i] \sigma_- \quad (10)$$

where $\alpha_\pm = \sqrt{a_1 a_2} \pm \frac{1}{\sqrt{a_1 a_2}}$ and $\alpha_0 = \sqrt{\frac{a_1}{a_2} + \frac{a_2}{a_1}}$. In a finite system, roots are $\beta_1, \beta_2 \approx a_1, a_2$ and $\beta_3, \beta_4 \approx b_1, b_2$, with the corresponding eigenmodes, up to $O(E)$, given by

$$\varphi_i = \begin{pmatrix} E \\ (a_i - b_1)(a_i - b_2) \end{pmatrix}; \varphi_{i+2} = \begin{pmatrix} (b_i - a_1)(b_i - a_2) \\ E \end{pmatrix}, \quad (11)$$

where $i = 1, 2$. Together with the hopping matrices $T_{\pm 1} = (a_1 a_2)^{\mp \frac{1}{2}} \sigma_+ + (b_1 b_2)^{\mp \frac{1}{2}} \sigma_-$ from $H_{\min}^{\text{PH}}(z)$, we can put $\text{Det } M = 0$, up to order $O(E^2)$, into the form

$$(a_1^l - a_2^l)(b_1^l - b_2^l) = E^2 \left(m_0(a_1^l a_2^l + b_1^l b_2^l) + \sum_{ij} m_{ij} a_i^l b_j^l \right), \quad (12)$$

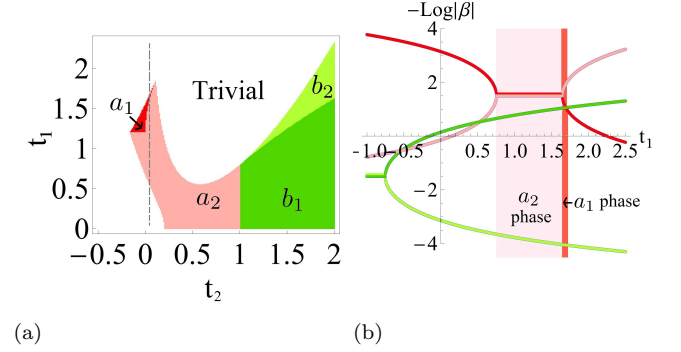


FIG. 3: a) Phase diagram of Hamiltonians described by Eq. 16 with different colors representing topological regimes with zero mode decay rate $-(\log |\beta|)^{-1}$ determined by $\beta = a_1, a_2, b_1$, or b_2 , respectively. b) For further illustration, we examine in the four $-\log |\beta|$ solutions the dashed line of (a) along $t_2 = 0.05$, with solutions $\beta = a_1, a_2, b_1$, and b_2 colored red, light red, dark green, and light green. From criterion 15, topological modes occur when no green (red) curve falls between two red (green) curves. Such regimes are colored translucent red and light red, respectively, corresponding to whether a_1 or a_2 determine the mode decay rate.

where m_0 and m_{ij} are coefficients independent of l . For a solution $\text{Det } M = 0$ to exist, both sides of Eq. 12 must scale similarly with l . Since the RHS is already suppressed by E^2 , the LHS cannot contain the most slowly decaying terms. Specifically, the pairs a_1, a_2 or b_1, b_2 *must* be the two β_μ ’s with largest magnitude, since they are absent in the LHS but not the RHS. Such con-

straints imposed by the scaling suppression from E^2 also appear in generic cases, and is guaranteed by the defective eigenspace of $H(z)$ (Eq. 9) at $E = 0$. With some effort, we can show that an isolated boundary zero mode exists only when the $r_a + r_b$ largest β_μ 's *do not* contain r_a members from $\{a_1, \dots, a_{p_a}\}$ and r_b members from $\{b_1, \dots, b_{p_b}\}$. The above constraints on the roots positions can now be elegantly recast in terms of the winding numbers

$$W_a(R) = \frac{1}{2\pi i} \oint_{|z|=R} d(\log a(z)) = \#Z_a(R) - \#P_a \quad (13)$$

$$W_b(R) = \frac{1}{2\pi i} \oint_{|z|=R} d(\log b(z)) = \#Z_b(R) - \#P_b \quad (14)$$

which give the number of zeros $\#Z_i(R)$ minus the number of poles $\#P_i$ encircled by the contour $|z| = R$, $R \in \mathbb{R}$. Evidently, $\#P_i = p_i - r_i$ does not depend on R , since the poles are always at $z = 0$. If R is chosen such that the contour $|z| = R$ excludes the r_a largest roots of $a(z)$, $W_a(R_a) = (p_a - r_a) - \#P_a = 0$. The same $|z| = R$, however, is not allowed to simultaneously exclude r_b roots of $b(z)$, for that would cause the $r_a + r_b$ excluded, i.e., largest roots, to be partitioned into r_a a_i 's and r_b b_i 's. Hence when $W_a(R) = 0$, we must have $W_b(R) < 0$, or vice versa. Thus a topological boundary zero mode exists if and only if

$$\exists R \in (0, \infty) \text{ such that } W_a(R)W_b(R) < 0 \quad (15)$$

The criterion 15 is a new result for non-Hermitian systems that does not require any customization of the contour[21]. Again, for the sake of illustration, we apply it to the subclass of models given by

$$H^{\text{PH}}[\gamma, t_{1/2}](z) \begin{pmatrix} 0 & t_1 - \gamma + z + t_2/z \\ t_1 + \gamma + 1/z + t_2 z & 0 \end{pmatrix}. \quad (16)$$

This yields the phase diagram in Fig. 3a, with the topological regime partitioned into four regions, depending on whether the zero mode decay length $-(\log |\beta|)^{-1}$ is given by the roots $a_{1,2} = (-t_1 - \gamma \pm \sqrt{(t_1 + \gamma)^2 - 4t_2})/(2t_2)$, or $b_{1,2} = (\gamma - t_1 \pm \sqrt{(t_1 - \gamma)^2 - 4t_2})/2$. Generically, the β_μ that dominates is the $(r_a + r_b + 1)$ th largest one - not necessarily the one corresponding to the imaginary gap (largest β_μ), which controls the hopping decays[34, 35], as illustrated in Fig. 3b, where the subleading slower decay rates are determined by the larger β_μ 's (Fig. 3c). For $t_2 = 0$ in (16), criterion 15 also easily reduces to the previously found formulations of a criterion for a topological phase[10, 21, 22] $|t_1^2 - \gamma^2| < 1$ viz. $a_1 = \infty, a_2 = -\frac{1}{t_1 + \gamma}, b_1 = \gamma - t_1$ and $b_2 = 0$. Even for a very complicated Hamiltonian, Criterion 15 can still be easily used after finding its zeros. As demonstrated in Fig. 4 for Hamiltonians with generic complex next-nearest neighbor hoppings, whether a zero mode exists depends on whether there exist a ring where $W_a > 0$ and $W_b < 0$

simultaneously (or vice-versa), i.e. where there are simultaneously less than r_a larger zeros of $a(z)$ and less than r_b smaller zeros of $b(z)$.

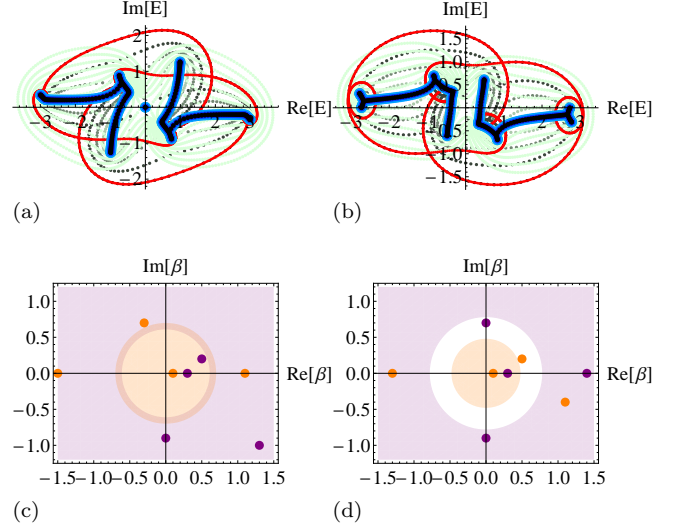


FIG. 4: Application of criterion 15 for a more complicated instance of (9) with $p_a = p_b = 4$ and $r_a = 3$, $r_b = 2$. Any model of (9), in terms of topology, is completely characterized by the roots of their $a(z)$ and $b(z)$, which are indicated by purple or orange dots in (c,d). Circles in the purple region ($W_a > 0$) enclose at least $q_a + 1 = p_a - r_a + 1 = 2$ purple roots, while circles in the orange region ($W_b < 0$) enclose fewer than $q_b + 1 = p_b - r_b + 1 = 2$ orange roots. In (a, c), the existence of a zero mode corresponds to the existence of an overlap region where $W_a > 0$ (purple) and $W_b < 0$ (orange). In (b,d), no such overlap exists, implying the absence of a topological mode.

Discussion – In this work, we have provided a rigorous treatment of boundary modes in non-Hermitian systems. We have demonstrated how the skin modes can be precisely characterized through an imaginary flux threading argument, and developed a new winding number criterion for 1D topological boundary modes. This criterion $W_a(R)W_b(R) < 0$ reduces to the simple statement of nontrivial winding $W_a(R)^2 > 0$ in the Hermitian case, where $W_b(R) = -W_a(R)$ and R can be taken to be unity. It represents a new addition to previously proposed non-Hermitian winding numbers $(W_a(R) \pm W_b(R))/2$, which captures the branch cut and eigenmode winding behavior, respectively[13, 21]. Our framework also reveals the intuition behind the extreme sensitivity of non-Hermitian system to the boundary: even in a large system, a small reduction in the boundary hopping $\sim e^{-\kappa l}$ can be equivalent to a large change in κ for the *entire* system.

Acknowledgements – We thank Zhong Wang, Xiao Zhang, Xiong Ye, Tobias Helbig and Tobias Hoff-

man for helpful comments. R.T. is supported by the European Research Council through ERC-StG-Thomale-TOPOLECTRICS-336012 and by DFG-SFB 1170 (project B04).

* calvin-lee@ihpc.a-star.edu.sg

- [1] F. D. M. Haldane, Phys. Rev. Lett. **61**, 2015 (1988).
- [2] M. Z. Hasan and C. L. Kane, Rev. Mod. Phys. **82**, 3045 (2010).
- [3] X.-L. Qi and S.-C. Zhang, Rev. Mod. Phys. **83**, 1057 (2011).
- [4] M. V. Berry, Proceedings of the Royal Society of London A: Mathematical, Physical and Engineering Sciences **392**, 45 (1984).
- [5] D. S. Sholl and J. A. Steckel, *Density Functional Theory* (Wiley, New Jersey, 2009).
- [6] M. Bukov, L. D'Alessio, and A. Polkovnikov, Advances in Physics **64**, 139 (2015).
- [7] R. El-Ganainy, K. G. Makris, M. Khajavikhan, Z. H. Musslimani, S. Rotter, and D. N. Christodoulides, Nature Physics **14**, 11 (2018).
- [8] M. V. Berry, Czechoslovak journal of physics **54**, 1039 (2004).
- [9] W. D. Heiss, Journal of Physics A: Mathematical and Theoretical **45**, 444016 (2012).
- [10] T. E. Lee, Phys. Rev. Lett. **116**, 133903 (2016).
- [11] W. Hu, H. Wang, P. P. Shum, and Y. Chong, Phys. Rev. B **95**, 184306 (2017).
- [12] V. Achilleos, G. Theocharis, O. Richoux, and V. Pagneux, Phys. Rev. B **95**, 144303 (2017).
- [13] H. Shen, B. Zhen, and L. Fu, Phys. Rev. Lett. **120**, 146402 (2018).
- [14] Q. Zhong, M. Khajavikhan, D. Christodoulides, and R. El-Ganainy, arXiv preprint arXiv:1805.07620 (2018).
- [15] X.-L. Zhang, S. Wang, B. Hou, and C. Chan, Physical Review X **8**, 021066 (2018).
- [16] B. Zhen, C. W. Hsu, Y. Igarashi, L. Lu, I. Kaminer, A. Pick, S.-L. Chua, J. D. Joannopoulos, and M. Soljačić, Nature **525**, 354 (2015).
- [17] J. Carlström and E. J. Bergholtz, arXiv preprint arXiv:1807.03330 (2018).
- [18] Z. Yang and J. Hu, arXiv preprint arXiv:1807.05661 (2018).
- [19] V. M. Alvarez, J. B. Vargas, and L. F. Torres, Phys. Rev. B **97**, 121401 (2018).
- [20] Y. Xiong, Journal of Physics Communications **2**, 035043 (2018).
- [21] S. Yao and Z. Wang, Phys. Rev. Lett. **121**, 086803 (2018).
- [22] F. K. Kunst, E. Edvardsson, J. C. Budich, and E. J. Bergholtz, Phys. Rev. Lett. **121**, 026808 (2018).
- [23] K. Kawabata, K. Shiozaki, and M. Ueda, arXiv preprint arXiv:1805.09632 (2018).
- [24] S. Yao, F. Song, and Z. Wang, arXiv preprint arXiv:1804.04672 (2018).
- [25] Z. Gong, Y. Ashida, K. Kawabata, K. Takasan, S. Higashikawa, and M. Ueda, arXiv preprint arXiv:1802.07964 (2018).
- [26] R. B. Laughlin, Phys. Rev. B **23**, 5632 (1981).
- [27] Q. Niu, Phys. Rev. Lett. **64**, 1812 (1990).
- [28] N. Hatano and D. R. Nelson, Phys. Rev. Lett. **77**, 570 (1996).
- [29] A. A. Soluyanov and D. Vanderbilt, Phys. Rev. B **83**, 035108 (2011).
- [30] C. H. Lee and P. Ye, Physical Review B **91**, 085119 (2015).
- [31] Y. Hatsugai and T. Fukui, Phys. Rev. B **94**, 041102 (2016).
- [32] S. Lieu, Physical Review B **97**, 045106 (2018).
- [33] C. Yin, H. Jiang, L. Li, R. Lü, and S. Chen, Physical Review A **97**, 052115 (2018).
- [34] C. H. Lee, D. P. Arovas, and R. Thomale, Phys. Rev. B **93**, 155155 (2016).
- [35] C. H. Lee, M. Claassen, and R. Thomale, Phys. Rev. B **96**, 165150 (2017).